

Iris-Biometric Comparators: Exploiting Comparison Scores towards an Optimal Alignment under Gaussian Assumption

Christian Rathgeb, Andreas Uhl, and Peter Wild*

Multimedia Signal Processing and Security Lab

Department of Computer Sciences, University of Salzburg, Austria

{crathgeb, uhl, pwild}@cosy.sbg.ac.at

Abstract

Iris-based systems guarantee a level of security and identity protection that is unparalleled by any other biometric. In past years numerous iris recognition algorithms have been proposed revealing impressive recognition rates. While the vast majority of research is focused on extracting highly discriminative feature vectors potential improvements in biometric comparators are commonly neglected. In this paper a new strategy for comparing binary biometric templates, in particular iris-codes, is presented. Instead of optimally aligning two iris-codes by maximizing the comparison score for several bit shifts utilizes the total series of comparison scores, avoiding any information loss. The soundness of the approach, which requires marginal additional computational effort, is confirmed by experiments applying two different iris-biometric feature extraction algorithms.

1. Introduction

Research confirms an extraordinarily high level of statistical reliability for iris recognition systems. Existing approaches show practical performance on diverse test sets, reporting recognition rates above 99% and equal error rates of less than 1% [1]. The majority of iris recognition algorithms extract binary feature vectors, *i.e.* iris-codes, applying the fractional Hamming distance to estimate distance scores between pairs of biometric templates. Alignment of biometric templates is achieved by a circular bit-shifting of iris-codes (to some degree), where the minimum obtained Hamming distance corresponds to an optimal alignment, as shown in Fig. 1. While most approaches to iris recognition algorithms focus on extracting highly discriminative iris-codes, potential improvements in the comparison stage are frequently neglected.

*supported by the Austrian Science Fund FWF, project no. L554-N15 and FIT-IT Trust in IT-Systems, project no. 819382.

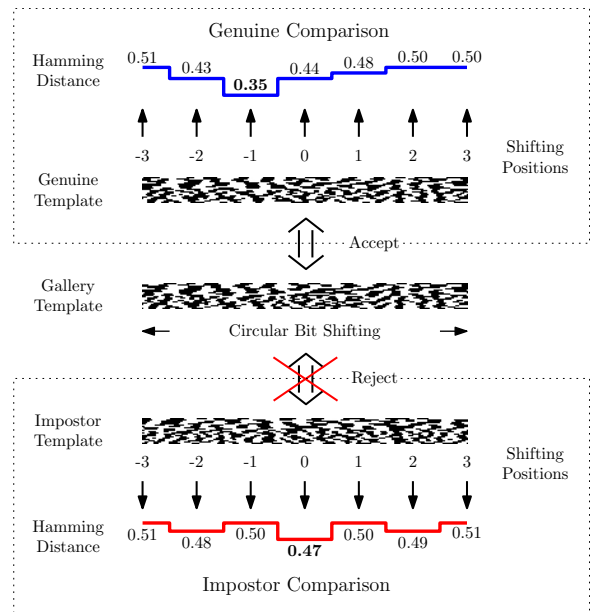


Figure 1. Template alignment in iris recognition: circular-shifting is performed to compensate for head tilts.

The contribution of this work is the proposal of a new comparison technique for binary biometric templates, in particular iris-codes. Since bits within binary biometric feature vectors are not mutually independent [2] (cf. Fig. 1) comparison scores consistently improve towards an optimal alignment, in case binary templates are extracted from a single subject. In contrast, intuitively a successive improvement (over several bit-shifts) is not expected to hold for comparisons of pairs of feature vectors obtained from different subjects. The proposed iris-biometric comparator utilizes these facts by fitting comparison scores to an algorithm-dependent Gaussian function, obtained from genuine comparisons (aligned at an optimal shifting position) within a training set. Experimental evaluations are carried out based on different iris-biometric feature extractors. Significant improvements with respect to recognition accuracy are achieved.

The remainder of this paper is organized as follows: in Section 2 related work is briefly discussed. Subsequently, the operation mode of the proposed comparison technique is described in detail in Section 3. Experimental results are presented in Section 4. Section 5 concludes the paper.

2. Related Work

Focusing on iris recognition, a binary representation of biometric features offers two major advantages: (1) rapid authentication (even in identification mode) and (2) compact storage of biometric templates. Comparisons between binary biometric feature vectors are commonly implemented by the simple Boolean exclusive-OR operator (XOR) applied to a pair of binary biometric feature vectors, masked (AND'ed) by both of their corresponding mask templates to prevent occlusions caused by eyelids or eyelashes from influencing comparisons. The XOR operator \oplus detects disagreement between any corresponding pair of bits, while the AND operator \cap ensures that the compared bits are both deemed to have been uncorrupted by noise. The norms ($\|\cdot\|$) of the resulting bit vector and of the AND'ed mask template are then measured in order to compute a fractional Hamming distance (HD) as a measure of the (dis-)similarity between pairs of binary feature vectors $\{\text{codeA}, \text{codeB}\}$ and the according mask bit vectors $\{\text{maskA}, \text{maskB}\}$ [2]:

$$HD = \frac{\|(\text{codeA} \oplus \text{codeB}) \cap \text{maskA} \cap \text{maskB}\|}{\|\text{maskA} \cap \text{maskB}\|}. \quad (1)$$

Apart from the fractional Hamming distance several other techniques of how to compare iris-codes have been proposed. To obtain a representative user-specific iris template during enrollment Davida *et al.* [3] and Ziauddin and Dailey [10] analyze several iris-codes. Davida *et al.* propose a majority decoding where the majority of bits is assigned to according bit positions in order to reduce Hamming distances between genuine iris-codes. Ziauddin and Dailey suggest to assign weights to each bit position, defining the stability of bits at according positions. Hollingsworth *et al.* [5] examined the consistency of bits in iris-codes resulting from different parts of the iris texture. The authors suggest to mask out so-called “fragile” bits for each user, where these bits are detected from several iris-code samples. In experimental results the authors achieve a significant performance gain. Obviously, applying more than one enrollment sample yields better recognition performance [4]. Uhl and Wild [9] have proposed the use of a constrained version of the Levenshtein distance to tolerate *e.g.* segmentation inaccuracies or non-linear deformations by employing inexact matching. Rathgeb *et al.* [8] estimate the shifting variation resulting from different shifting positions, *i.e.* the authors

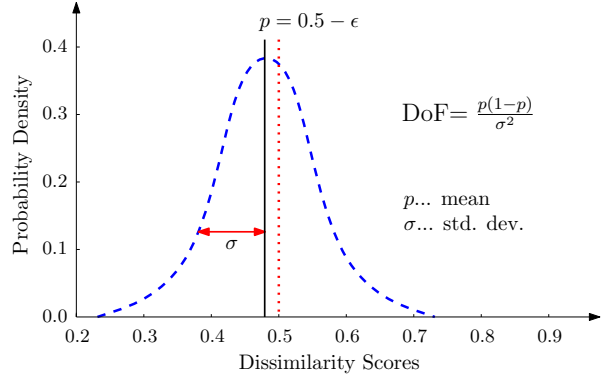


Figure 2. Binomial distribution of Hamming distances between different pairs of binary biometric feature vectors.

propose a score level fusion of maximum and minimum obtained Hamming distance scores obtaining a significant improvement regarding recognition accuracy.

3. Exploiting Preliminary Comparison Scores

A common way to estimate the average entropy of biometric feature vectors is to measure the provided “degrees-of-freedom” which are defined by $d = p(1 - p)/\sigma^2$, where p is the mean HD and σ^2 the corresponding variance between comparisons of different pairs of binary feature vectors, shown in Fig. 2. In case all bits of each binary feature vector of length n would be mutually independent, comparisons of pairs of different feature vectors would yield a binomial distribution,

$$\mathcal{B}(n, k) = \binom{n}{k} p^k (1 - p)^{n-k} = \binom{n}{k} 0.5^n \quad (2)$$

and the expectation of the Hamming distance would be $\mathbb{E}(HD(\text{codeA}, \text{codeB})) = 1/n \cdot \mathbb{E}(X \oplus Y) = np \cdot 1/n = p = 0.5$, where X and Y are two independent random variables in $\{0, 1\}$. In reality reasonable parts of feature vectors correlate. As a consequence p decreases to $0.5 - \epsilon$ while Hamming distances remain binomially distributed with a reduction in n .

Based on the fact that not all bits in iris-codes are mutually independent (e.g. in [2] feature vectors of 2048 bits exhibit 249 degrees of freedom) comparison scores are expected to improve until an optimal alignment is reached, which corresponds to a minimal obtained Hamming distance. In case two identical iris-codes are compared resulting scores constantly decrease until $0.5 - \epsilon$ at a certain shifting position (in both directions). These logical justifiable assumptions motivate a tracking of progressions in observed comparison scores. In the following subsection the training stage and the proposed comparison technique are described in detail.

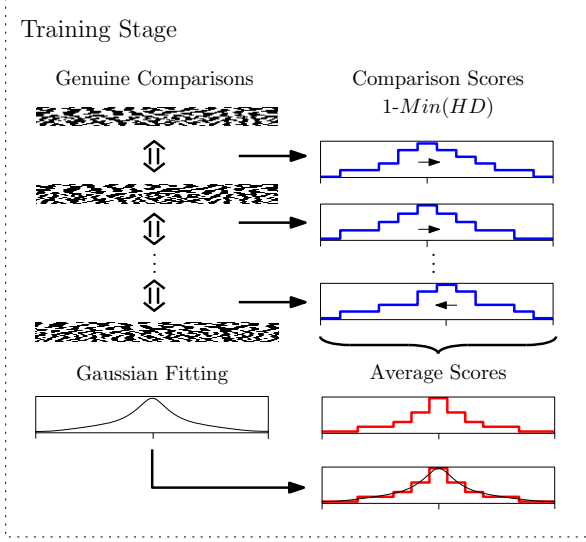


Figure 3. Training stage: scores obtained from genuine comparisons within a training set are modeled applying a Gaussian.

3.1. Training Stage

In the proposed system a training set of iris-codes is applied to model an average algorithm-dependent distribution of comparison scores at a certain alignment. For this purpose all genuine comparisons within the training set are performed. Let $s(\text{codeA}, i)$ denote the shifting of an iris-code codeA by $i \in I_n = \{z \in \mathbb{Z} : |z| \leq n\}$ bits, then the minimal Hamming distance of two iris-codes is defined as,

$$\text{MinHD}(\text{codeA}, \text{codeB}) = \min_{i \in I_n} \left(\text{HD}(\text{codeA}, s(\text{codeB}, i)) \right). \quad (3)$$

Once an optimal alignment is detected for each pair of iris-codes (of a single subject) the progression of scores with respect to the optimal alignment is tracked in an histogram within an adequate range (e.g. ± 8 bit shifts in each direction). Based on all tracked comparison scores an average algorithm-dependent score is estimated at certain shifting positions with reference to an optimal alignment.

It is found that average distributions of comparison scores, in particular $1 - \text{MinHD}$, at certain shifting positions can be approximated by a Gaussian function,

$$G(k, i) = t + \frac{1}{\sigma\sqrt{2\pi}} e^{-(k-i)^2/(2\sigma^2)} \quad (4)$$

where t represents the decision threshold of the system and i refers to the optimal shifting position. An adequate Gaussian can be established by manual fitting or by applying any systematic approach, e.g. nonlinear least squares fitting. The proposed training stage is schematically illustrated in Fig. 3.

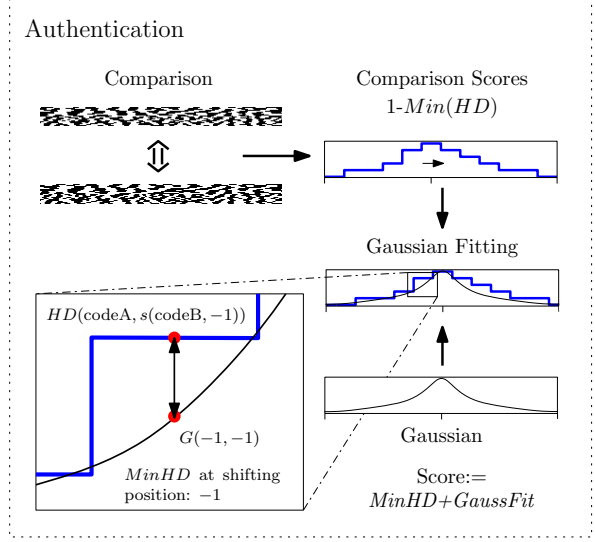


Figure 4. Authentication: scores at different shifting positions are sequentially fitted to a Gaussian obtained during the training stage.

3.2. Proposed Comparison Technique

At the time of authentication the deviation of comparison scores to the corresponding Gaussian (estimated at training stage) is measured at different shifting positions. For this purpose the function *GaussFit* is defined, which calculates the quadratic error of the comparison score between two iris codes codeA and codeB at a distinct shifting position k to a Gaussian G ,

$$\text{GaussFit}(\text{codeA}, \text{codeB}, k) = \left(1 - \text{HD}(\text{codeA}, s(\text{codeB}, k)) - G(k, i) \right)^2. \quad (5)$$

The deviation is estimated for distinct shifting positions $k \in K_n = \{z \in \mathbb{Z} : |z| \leq n\}$ based on the optimal shift i in order to calculate the final fitting score, denoted by $\text{GaussFit}(\text{codeA}, \text{codeB})$. The final score is defined by $\|\sum_{k=-n}^n \text{GaussFit}(\text{codeA}, \text{codeB}, k)\|$, the sum of all quadratic errors which is normalized to the range $[0, 1]$. Normalization is performed based on minimum and maximum values which are estimated from the applied training set (during experiments occurring outliers are set to 0 or 1, respectively). Subsequently, the resulting fitting score is combined with the *MinHD* comparator applying sum rule fusion. The proposed comparator, denoted by *MinHD+GaussFit*, is defined by,

$$\text{MinHD+GaussFit}(\text{codeA}, \text{codeB}) = \left(\text{MinHD}(\text{codeA}, \text{codeB}) + \text{GaussFit}(\text{codeA}, \text{codeB}) \right) / 2. \quad (6)$$

In contrast to the *MinHD* comparator the proposed comparator additionally tracks improvements of comparison

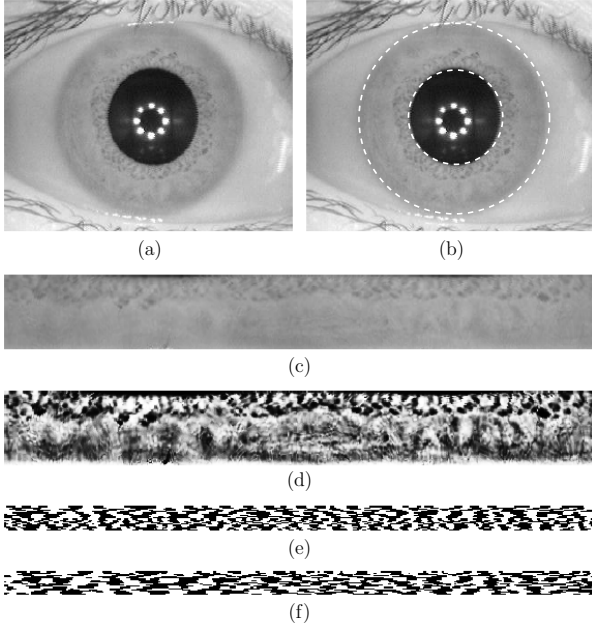


Figure 5. Preprocessing and feature extraction: (a) image of eye (b) detection of pupil and iris (c) unwrapped and (d) preprocessed iris texture, iris-code of (e) Ma *et al.* and (f) Masek.

scores towards the estimation of an optimal alignment, which is likely for genuine comparisons. On the other hand the presented approach is expected to increase dissimilarity between pairs of iris-codes extracted from different subject where Gaussian progressions in comparison scores are rather unlikely. Obviously, the proposed technique requires additional computational effort over the *MinHD* comparator, however, extra cost is kept low compared to other proposed approaches (*e.g.* [10, 9]). Fig. 4 illustrates the operation mode of the proposed comparison technique.

4. Experimental Studies

4.1. Experimental Setup

Experiments are carried out on the CASIA-v3-Interval iris database¹. The database consists of good quality 320×280 pixel NIR illuminated indoor images, a sample image is shown in Fig. 5 (a). At preprocessing the iris of a given sample image is detected, un-wrapped to a rectangular texture of 512×64 pixel, and lighting across the texture is normalized as shown in Fig. 5 (b)-(d).

In the feature extraction stage custom implementations of two different algorithms extracting binary iris-codes are employed. The first one was proposed by Ma *et al.* [6]. Within this approach the texture is divided into 10 stripes to obtain 5 one-dimensional signals, each one averaged from the pixels of 5 adjacent rows, hence, the upper 512×50 pixel of preprocessed iris textures are analyzed. A dyadic

Algorithm	p	σ	DoF (bit)
Ma <i>et al.</i> [6]	0.4965	0.0143	1232
Masek [7]	0.4958	0.0202	612

Table 1. Benchmark values of feature extraction algorithms.

wavelet transform is then performed on each of the resulting 10 signals, and two fixed subbands are selected from each transform resulting in a total number of 20 subbands. In each subband all local minima and maxima above a adequate threshold are located, and a bit-code alternating between 0 and 1 at each extreme point is extracted. Using 512 bits per signal, the final code is then $512 \times 20 = 10240$ bit. The second feature extraction method follows an implementation by Masek [7] in which filters obtained from a Log-Gabor function are applied. Here a row-wise convolution with a complex Log-Gabor filter is performed on the texture pixels. The phase angle of the resulting complex value for each pixel is discretized into 2 bits. To have a code comparable to the first algorithm, we use the same texture size and row-averaging into 10 signals prior to applying the one-dimensional Log-Gabor filter. The 2 bits of phase information are used to generate a binary code, which therefore is again $512 \times 20 = 10240$ bit. Sample iris-codes of both algorithms are shown in Fig. 5 (e)-(f).

4.2. Performance Evaluation

For both feature extraction methods the binomial distribution of Hamming distances between different pairs of iris-code are plotted in Fig. 6 (a). The according means, standard deviations, degrees of freedom are summarized in Table 1 (iris-codes extracted by the algorithm of Ma *et al.* exhibit twice as much degrees of freedom compared to the feature extraction of Masek). At training stage all genuine comparisons between pairs of iris-codes obtained from the first 10 subjects of the database are performed. The resulting distribution of comparison scores according to a detected minimal Hamming distance are plotted in Fig. 6 (b)-(c). For the algorithm of Ma *et al.* and Masek resulting distributions are approximated with a Gaussians, defined by standard deviations $\sigma=1.5$ and $\sigma=1.6$, respectively.

Recognition accuracy is evaluated in terms of genuine acceptance rate (GAR) at a certain false acceptance rate (FAR). The GAR defines the proportion of verification transactions with truthful claims of identity that are correctly confirmed, and the FAR defines the proportion of verification transactions with wrongful claims of identity that are incorrectly confirmed (ISO/IEC FDIS 19795-1). As score distributions overlap the equal error rate (EER) of the system is defined. At all authentication attempts 8 circular bit-shifts are performed in each direction for both feature extraction methods and proposed comparators.

For the feature extraction of Ma *et al.* and Masek the resulting receiver operation characteristics (ROCs) are plotted in Fig. 7. As can be seen, for both feature extrac-

¹The Center of Biometrics and Security Research, CASIA Iris Image Database, <http://www.sinobiometrics.com>

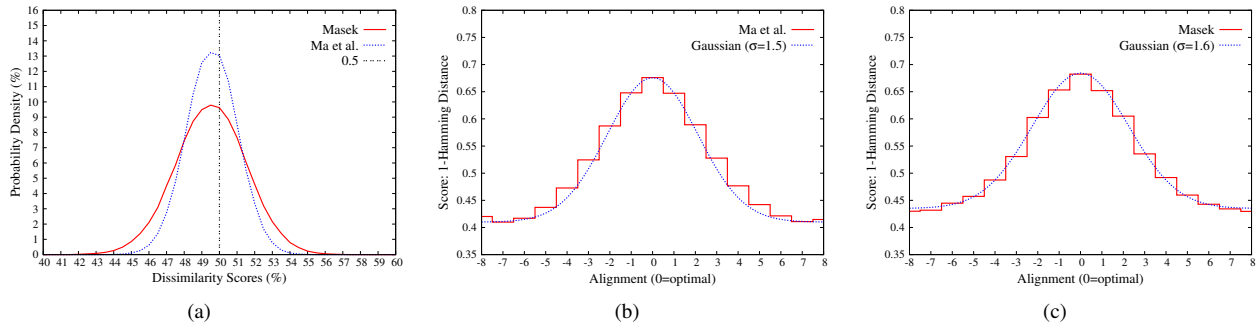


Figure 6. (a) Binomial distributions of Hamming distances between different pairs of feature vectors for both feature extraction algorithms and distributions of comparison scores according to a certain optimal alignment approximated by Gaussians for (b) Ma *et al.* and (c) Masek.

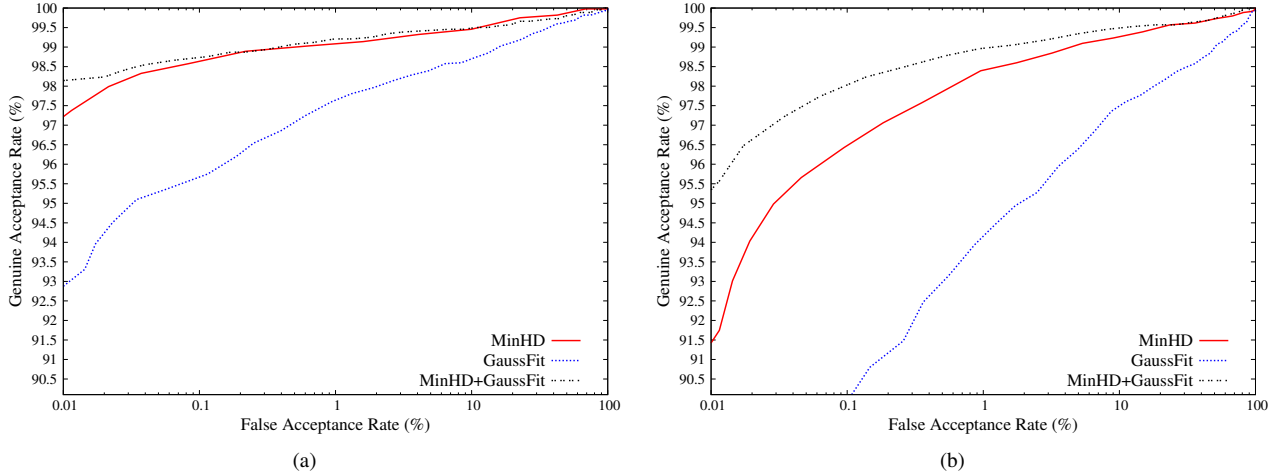


Figure 7. ROC curves for the presented comparison techniques applying the feature extraction method of (a) Ma *et al.* and (b) Masek.

tion methods, *MinHD+GaussFit* reveals an improved performance over *MinHD* while *GaussFit* shows rather unpractical rates. Despite this weak performance of *GaussFit*, measured scores are suitable in a fusion with *MinHD* to improve the total combined score. Applying the *MinHD* comparator EER of 0.89% and 1.29% and GARs of 97.98% and 91.74% at FARs of 0.01% are achieved for the algorithm of Ma *et al.* and Masek, respectively. With respect to the *GaussFit* comparator accuracy significantly decreases, e.g. for the feature extraction of Masek an EER of 4.07% and a GAR of 83.20% at a FAR of 0.01% is obtained. However, a fusion of both comparators, *MinHD+GaussFit*, yields an EER of 0.73% for the algorithm of Ma *et al.* and an EER of 0.94% for the algorithm of Masek, since in the fusion scenario additional information about score progressions towards an optimal alignment is added. At FARs of 0.01% GARs of 98.35% and 95.56% are achieved for both feature extraction methods, respectively. All experimental results with respect to obtained EERs and GARs are summarized in Table 2 and Table 3.

The intra-class and inter-class score distributions for the algorithm of Ma *et al.* applying the *MinHD* comparator and the proposed *MinHD+GaussFit* comparator are plotted in Fig. 8. Applying the proposed comparator score distributions are further separated leading to an improved

EER (%)	<i>MinHD</i>	<i>GaussFit</i>	<i>MinHD+GaussFit</i>
Ma <i>et al.</i> [6]	0.89	1.89	0.73
Masek [7]	1.29	4.07	0.94

Table 2. Equal error rates for the presented comparison techniques.

GAR (%)	<i>MinHD</i>	<i>GaussFit</i>	<i>MinHD+GaussFit</i>
Ma <i>et al.</i> [6]	97.98	92.69	98.35
Masek [7]	91.74	83.20	95.56

Table 3. Genuine acceptance rates for the presented comparison techniques (at FAR=0.01%).

recognition accuracy. The same characteristics are observed for the feature extraction method of Masek, score distributions for the *MinHD* comparator and the proposed *MinHD+GaussFit* comparator are shown in Fig. 9. Focusing on the *MinHD+GaussFit* comparator, for both feature extraction techniques the vast majority of genuine comparison scores is further reduced while standard deviation of binomial distributions of impostor scores increase.

5. Conclusion

In this paper an improved iris-biometric comparator is proposed. The presented comparison technique utilizes the total series comparison scores which are estimated at the time of template alignment, *i.e.* information loss is avoided.

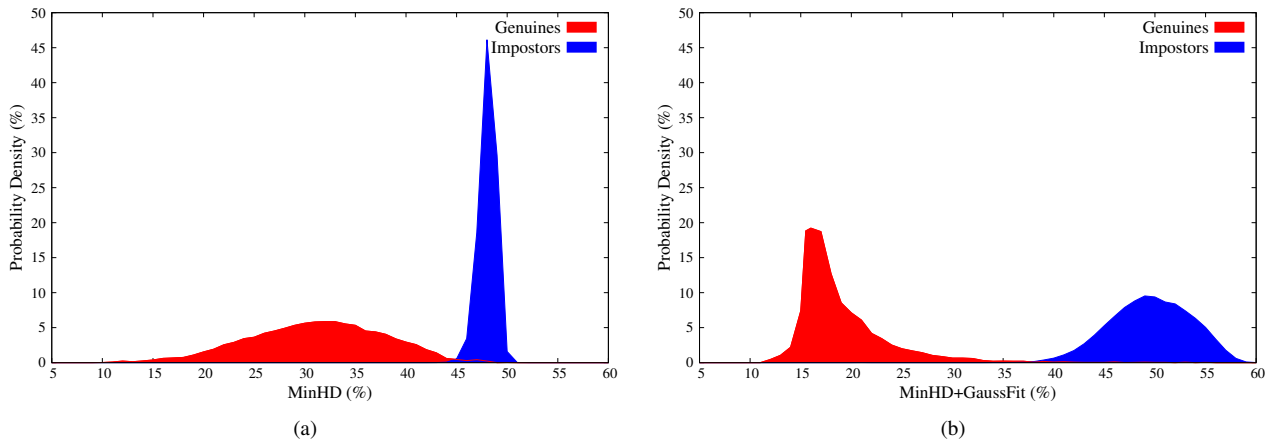


Figure 8. Genuine and impostor score distribution applying (a) *MinHD* and (b) *MinHD+GaussFit* for the algorithm of Ma *et al.*

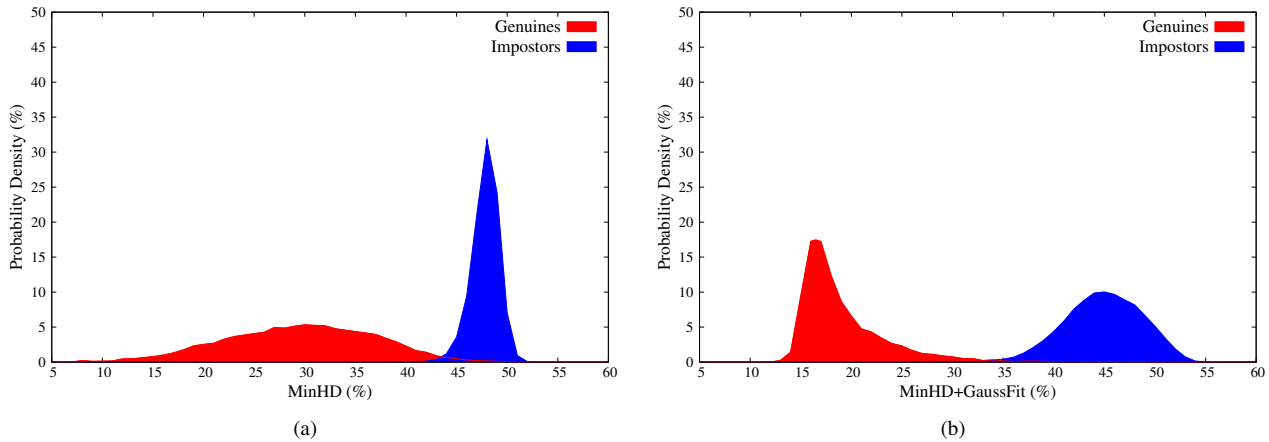


Figure 9. Genuine and impostor score distribution applying (a) *MinHD* and (b) *MinHD+GaussFit* for the algorithm of Masek.

Since bits in iris-codes are not mutually independent successive improvements within scores are observed in case of genuine comparisons. From a training set of iris-codes distributions of comparison scores according to an estimated optimal alignment are modeled by a Gaussian distribution. At authentication the entire set of scores is fitted onto an algorithm-dependent Gaussian and the normalized fitting score is fused with the minimal obtained Hamming distance. Experiments are carried out for different iris biometric feature extraction methods achieving significant improvements in recognition accuracy (under negligible additional computational cost) confirming the soundness of the proposed technique.

References

- [1] K. W. Bowyer, K. Hollingsworth, and P. J. Flynn. Image understanding for iris biometrics: A survey. *Computer Vision and Image Understanding*, 110(2):281 – 307, 2008.
- [2] J. Daugman. The importance of being random: statistical principles of iris recognition. *Pattern Recognition*, 36(2):279 – 291, 2003.
- [3] G. Davida, Y. Frankel, and B. Matt. On enabling secure applications through off-line biometric identification. *Proc. of IEEE, Symp. on Security and Privacy*, pages 148–157, 1998.
- [4] Y. Du. Using 2d log-gabor spatial filters for iris recognition. In *Proc. of the SPIE 6202: Biometric Technology for Human Identification III*, pages 62020:F1–F8, 2006.
- [5] K. P. Hollingsworth, K. W. Bowyer, and P. J. Flynn. The best bits in an iris code. *IEEE Transactions on Pattern Analysis and Machine Intelligence*, 31(6):964–973, 2009.
- [6] L. Ma, T. Tan, Y. Wang, and D. Zhang. Efficient Iris Recognition by Characterizing Key Local Variations. *IEEE Transactions on Image Processing*, 13(6):739–750, 2004.
- [7] L. Masek. Recognition of human iris patterns for biometric identification. Master’s thesis, University of Western Australia, 2003.
- [8] C. Rathgeb, A. Uhl, and P. Wild. Shifting score fusion: On exploiting shifting variation in iris recognition. In *Proc. of the 26th ACM Symposium On Applied Computing (SAC’11)*, pages 1–5, 2011.
- [9] A. Uhl and P. Wild. Enhancing iris matching using levenstein distance with alignment constraints. In *Proc. of the 6th Int. Symp. on Advances in Visual Computing (ISVC’10)*, pages 469–479, 2010.
- [10] S. Ziauddin and M. Dailey. Iris recognition performance enhancement using weighted majority voting. In *Proc. of the 15th Int. Conf. on Image Processing (ICIP ’08)*, pages 277–280, 2008.